



## Effects of Li doping on H-diffusion in MgH<sub>2</sub>: A first-principles study

Wenmei Ming, Zhigang Zak Fang, and Feng Liu

Citation: [Journal of Applied Physics](#) **114**, 243502 (2013); doi: 10.1063/1.4853055

View online: <http://dx.doi.org/10.1063/1.4853055>

View Table of Contents: <http://scitation.aip.org/content/aip/journal/jap/114/24?ver=pdfcov>

Published by the [AIP Publishing](#)

---



## Re-register for Table of Content Alerts

Create a profile.



Sign up today!



## Effects of Li doping on H-diffusion in MgH<sub>2</sub>: A first-principles study

Wenmei Ming,<sup>1</sup> Zhigang Zak Fang,<sup>2</sup> and Feng Liu<sup>1,a)</sup>

<sup>1</sup>Department of Materials Science and Engineering, University of Utah, Salt Lake City, Utah 84112, USA

<sup>2</sup>Department of Metallurgical Engineering, University of Utah, 135 South 1460 East, Room 412, Salt Lake City, Utah 84112-0114, USA

(Received 5 November 2013; accepted 6 December 2013; published online 23 December 2013)

The effects of Li doping in MgH<sub>2</sub> on H-diffusion process are investigated, using first-principles calculations. We have identified two key effects: (1) The concentration of H vacancy in the +1 charge state ( $V_H^{+1}$ ) can increase by several orders of magnitude upon Li doping, which significantly increases the vacancy mediated H diffusion rate. It is caused by the preferred charge states of substitutional Li in the -1 state ( $Li_{Mg}^{-1}$ ) and of interstitial Li in the +1 state ( $Li_i^{+1}$ ), which indirectly reduce the formation energy of  $V_H^{+1}$  by up to 0.39 eV depending on the position of Fermi energy. (2) The interaction between  $V_H^{+1}$  and  $Li_{Mg}^{-1}$  is found to be attractive with a binding energy of 0.55 eV, which immobilizes the  $V_H^{+1}$  next to  $Li_{Mg}^{-1}$  at high Li doping concentration. As a result, the competition between these two effects leads to large enhancement of H diffusion at low Li doping concentration due to the increased H-vacancy concentration, but only limited enhancement at high Li concentration due to the immobilization of H vacancies by too many Li. © 2013 AIP Publishing LLC.

[<http://dx.doi.org/10.1063/1.4853055>]

### I. INTRODUCTION

Light metal hydride MgH<sub>2</sub> is one of the most promising hydrogen-storage materials for on-board clean-fuel application, because it has both high gravimetric (7.7 wt. %) and volumetric densities ( $6.7 \times 10^{22}$  H/cm<sup>3</sup>).<sup>1</sup> However, their dehydrogenation process is too slow to be practically useful, and for bulk materials as high as about 300 K above room temperature is required to obtain an equilibrium H<sub>2</sub> pressure of 1 bar.<sup>1-4</sup> Such poor dehydrogenation kinetics are primarily due to the strong ionic bonding between Mg and H and large enthalpy of formation of MgH<sub>2</sub> (~75 KJ/molH<sub>2</sub>), as evidenced by both experiments<sup>5-7</sup> and first-principles calculations.<sup>8,9</sup> Various attempts have been made to help facilitate dehydrogenation process. For example, to improve the kinetics, ball milling processing<sup>10,11</sup> has been used to shorten the diffusion length, doping of transition metals<sup>10-12</sup> were adopted to reduce the strength of H-Mg bond, and applying tensile stress was tried to weaken the Mg-H stability.<sup>2,13</sup>

On the other hand, doping has been known to enhance H diffusion in metal hydrides, which is usually mediated by H vacancy, by inducing a higher concentration of H-vacancy.<sup>14-19</sup> For example, Van de Walle *et al.* recognized that in certain charged state, Zr(Ti) can enhance the dehydrogenation kinetics of NaAlH<sub>4</sub>,<sup>14</sup> because the formation energy of H-vacancy is decreased upon doping. In particular, when the H-vacancy is charged, its formation energy depends on the position of Fermi energy; and conversely, selective doping of the hydride with impurities that take different charged states will tune the Fermi energy with respect to the dopant-free system. And the shift of Fermi energy can result in a decrease of H-vacancy formation energy depending on the sign of the H-vacancy charge state. Consequently, the concentration of H-vacancy will increase to enhance the vacancy-mediated H diffusion.

In this work, we investigated the effects of Li doping on H diffusion in MgH<sub>2</sub>. One important reason that we chose Li is because it is a lighter metal than Mg, so that it will not degrade the high H gravimetric density. We focused on the effects of charge state of Li impurity and H-vacancy, as recognized before in other systems,<sup>14</sup> but also went beyond the previous works by taking into account the effects of interaction between the charged impurities and defects. In many previous studies of the charged-impurity-enhanced H diffusion,<sup>14-19</sup> it implicitly assumed no interaction between the dopant and defect. This might be true in the limit of low doping concentration and weak defect-dopant interaction, but unlikely at high doping concentration. Especially, if there is an attractive impurity-defect interaction, such as the binding between the Li-dopant and H-vacancy in MgH<sub>2</sub> as shown by Smith *et al.*,<sup>20</sup> the impurity may immobilize the H-vacancy, counteracting the enhancement effect of H-vacancy on H diffusion.

Therefore, by taking into account the binding between Li and H-vacancy and its dependence on the charge states of Li and H-vacancy, we have systematically studied the effects of Li doping on H diffusion in MgH<sub>2</sub> as a function of Li concentration. We have determined the favored charge states of Li by calculating its formation energy as a function of Fermi energy, the equilibrium concentration of H vacancies by calculating the H vacancy formation energy as a function of Li doping concentration, and the percentage of immobilized H-vacancies by calculating the binding energies between H-vacancy and Li-dopant. We have also calculated the diffusion barrier of H-vacancy in the presence of Li dopant.

### II. CALCULATION DETAILS

Our first principles calculations based on density functional theory (DFT) were conducted using projector augment wave pseudopotential (PAW)<sup>21</sup> with the generalized gradient approximation (GGA)<sup>22</sup> to the exchange-correlation functional, as implemented in VASP package.<sup>23</sup> Supercell

<sup>a)</sup>Author to whom correspondence should be addressed. Electronic mail: [fliu@eng.utah.edu](mailto:fliu@eng.utah.edu)

technique was used to calculate the formation energy of defects and dopants, interaction energy and diffusion barrier. We used a supercell comprised of  $3 \times 3 \times 4$  primitive  $\text{MgH}_2$  rutile unit cells with the dimensions of  $13.481 \times 13.481 \times 12.012 \text{ \AA}^3$ . 400 eV energy cutoff and  $2 \times 2 \times 2$  k-mesh were used for wavefunction expansion and k-space integration, respectively. All the structures were relaxed in terms of internal atomic coordinates using conjugate gradient method until the force exerted on each atom was smaller than  $0.005 \text{ eV/\AA}^3$ . The charged system was simulated by adding to or removing from the system electrons with a compensating uniform opposite charge background. Diffusion barrier was calculated using the nudged elastic band method.<sup>24</sup>

The formation energy  $E^f(X^q)$  of defect or dopant ( $X$ ) with charge  $q$  was computed according to Ref. 25

$$\Delta E^f(X^q) = E_{tot}(X^q) - E_{tot}(bulk) - \sum_i n_i \mu_i + q(E_F + E_\nu + \Delta V), \quad (1)$$

where  $E_{tot}(bulk)$  and  $E_{tot}(X^q)$  are the total energies of supercell for pure  $\text{MgH}_2$  and for  $\text{MgH}_2$  containing defect or dopant ( $X^q$ ), respectively.  $E_\nu$  is chosen to be the valence band maximum (VBM) energy.  $E_F$  is the Fermi energy with respect to  $E_\nu$ .  $\Delta V$  is additional electrostatic energy alignment due to different energy references between the defect-containing structure and defect-free structure.  $i$  denotes H-defect or dopant Li and  $n_i$  is the number of species  $i$  in the supercell.  $\mu_i$  is the chemical potential of species  $i$ . In low concentration limit, the equilibrium defect concentration can be related to the formation energy using

$$C = N \exp(-\Delta E^f/k_B T), \quad (2)$$

where  $N$  is the number of sites that can be occupied by defect,  $k_B$  is Boltzman constant, and  $T$  is temperature in K.

For the chemical potential  $\mu_i$ , the externally added dopant Li is assumed to have its bulk chemical potential  $E_{Li}(bulk)$ . The chemical potential of H,  $\mu_H$  is in between  $\frac{1}{2}E(H_2) + \frac{1}{2}\Delta H_f(\text{MgH}_2)$  (H-poor condition) and  $\frac{1}{2}E(H_2)$  (H-rich condition), considering thermodynamic equilibrium between  $\text{MgH}_2$ , Mg, and  $\text{H}_2$ .  $\Delta H_f(\text{MgH}_2)$  is enthalpy of formation of  $\text{MgH}_2$ ,  $E(H_2)$  is the energy of hydrogen molecule at 0 K. Similarly, the chemical potential of Mg is in between  $E(bulk \text{ Mg})$  and  $E(bulk \text{ Mg}) + \Delta H_f(\text{MgH}_2)$ . We specifically considered two extreme cases: H poor condition and H rich condition.

### III. RESULTS AND DISCUSSION

First, we calculated the formation energy of native defects: H-vacancy ( $V_H$  with charge  $-1, 0, +1$ ) and interstitial H ( $H_i$  with charge  $-1, 0, +1$ ). The preferred defects are  $V_H^{-1}$  and  $V_H^{+1}$  in H-poor condition, and  $V_H^{+1}$  and  $H_i^{-1}$  in H-rich condition, respectively. Charge neutrality condition requires Fermi-energy to be 2.85 eV and 2.65 eV for the H-poor condition and H-poor condition, respectively. These results are in good agreement with those for  $\text{MgH}_2$  in

TABLE I. The formation energy ( $\Delta E^f$ ) and concentration ( $C$ ) of relevant H-defects without (a) and with (b) dopant Li, at  $T = 400 \text{ K}$ .

	H-poor		H-rich	
	$V_H^+$	$V_H^-$	$V_H^+$	$H_i^-$
$\Delta E^f(\text{eV})^a$	1.225	1.225	1.358	1.358
$C(\text{cm}^{-3})^a$	$2.5 \times 10^7$	$2.5 \times 10^7$	$5.3 \times 10^5$	$5.3 \times 10^5$
$\Delta E^f(\text{eV})^b$	0.975	1.475	0.968	1.748
$C(\text{cm}^{-3})^b$	$3.5 \times 10^{10}$	$1.772 \times 10^4$	$4.13 \times 10^{10}$	6.5

Ref. 17. In Table I, we give an estimate of the concentration for the favored H-defects from Eq. (2).

In order to study how the formation energies of the H-related defects are affected by Li doping, we then calculated the formation energy for both substitutional Li configuration ( $\text{Li}_{Mg}$ ) and interstitial Li configuration ( $\text{Li}_i$ ) in the  $(-1, 0, +1)$  charge states. As shown in Figure 1 for both H-poor and H-rich conditions,  $\text{Li}_{Mg}^{-1}$  is more stable than  $\text{Li}_{Mg}^0$  and  $\text{Li}_{Mg}^{+1}$  in almost the whole range of Fermi energy in the gap except very close to the VBM. While  $\text{Li}_i^{+1}$  is more stable than other two charge states in almost the whole range of Fermi energy in the gap except very close to conduction band minimum (CBM). This indicates that the defect level remains close to the VBM and CBM for  $\text{Li}_{Mg}$  and  $\text{Li}_i$ , respectively (see Ref. 26 for similar behavior of native defects in anatase  $\text{TiO}_2$ ). Under the charge-neutrality

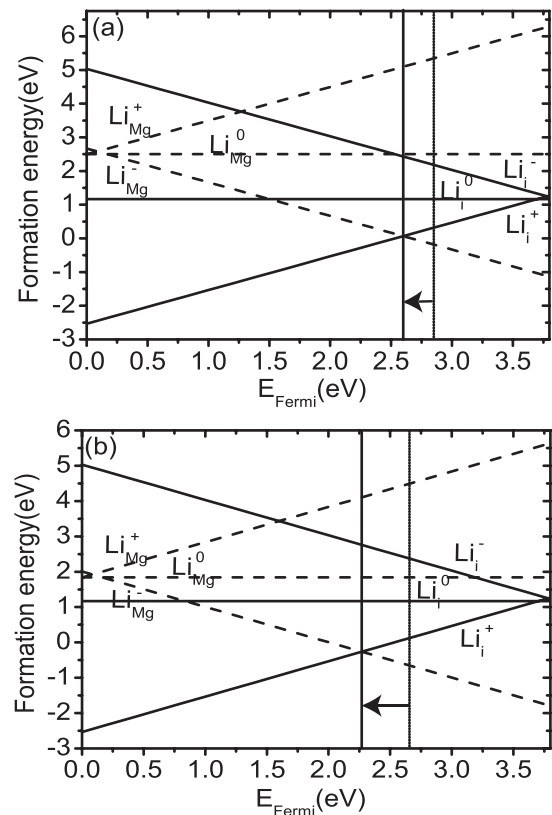


FIG. 1. Formation energy of Li-dopant in  $\text{MgH}_2$ : (a) H-poor condition, (b) H-rich condition. The vertical solid and dashed lines indicate the Fermi energy in  $\text{MgH}_2$  with and without Li, respectively.  $E_{Fermi} = 0 \text{ eV}$  corresponds to the VBM and  $E_{Fermi} = 3.8 \text{ eV}$  corresponds to the CBM.

condition, the Fermi energy of the Li-doped system (vertical solid lines) is shifted to the left by 0.25 eV (Fig. 1(a)) and 0.39 eV (Fig. 1(b)) with respect to the Fermi energy of the undoped system (vertical dashed lines) for the H-poor and H-rich conditions, respectively, assuming the concentration of dopant Li is much higher than that of H-defects so that the  $\text{Li}_i^{+1}$  and  $\text{Li}_{\text{Mg}}^{-1}$  are the dominant charged dopants to maintain the charge-neutrality condition. The Fermi energy in both situations is deep inside the band gap. Thus, the thermally excited free carriers in both valence and conduction band are negligible. The consequence of the shift of Fermi energy is that the formation energy of  $\text{V}_H^{+1}$  is reduced by 0.25 eV and 0.39 eV under the H-poor and H-rich conditions, respectively, according to Eq. (1). And the opposite effect happens to  $\text{V}_H^{-1}$  and  $\text{H}_i^{-1}$ : their formation energy is increased by 0.25 eV and 0.39 eV, respectively. As shown in Table I, at 400 K the concentration of  $\text{V}_H^{+1}$  in the Li-doped system is  $1.40 \times 10^3$  and  $8.12 \times 10^4$  times larger than that in the undoped system under the H-poor and H-rich conditions, respectively. On the contrary, the concentration of  $\text{H}_i^{-1}$  in the Li-doped system is  $\sim 10^5$  and  $\sim 5 \times 10^7$  times lower than that in the undoped system under the H-poor and H-rich conditions, respectively.

A previous calculation<sup>18</sup> showed that in the undoped  $\text{MgH}_2$ , the diffusion barrier of  $\text{V}_H^{+1}$  is 0.25 eV smaller than that of  $\text{V}_H^{-1}$  under the H-poor condition, and the diffusion barrier of  $\text{V}_H^{+1}$  is 0.36 eV higher than that of  $\text{H}_i^{-1}$  under the H-rich condition. This means that without Li doping, the  $\text{V}_H^{+1}$  is the dominant diffusing species under the H-poor condition, while the  $\text{H}_i^{-1}$  is the dominant diffusing species under the H-rich condition. Our calculations show that upon Li doping, the formation energy of  $\text{V}_H^{+1}$  is decreased by 0.25 eV under that H-poor condition, while that of  $\text{H}_i^{-1}$  is increased by 0.39 eV under H-rich condition. Because the H-related defect diffusion is determined by the activation barrier, which is the sum of the diffusion barrier and the formation energy. The  $\text{V}_H^{+1}$  remains the dominant diffusing species under the H-poor condition because its formation energy is decreased, leading to a lower activation barrier. In contrast, the  $\text{H}_i^{-1}$  becomes the less favorable diffusing species under the H-rich condition because its formation energy is increased, leading to a higher activation barrier. Consequently, the Li doping makes the  $\text{V}_H^{+1}$  the dominant diffusion species in the whole range of H chemical potential.

We note that we have neglected entropy contribution in our analysis. Usually, this is a good approximation because the contribution due to the entropy difference is much smaller than the contribution due to the total energy difference. Of course, more accurate results can be obtained by calculating the phonon spectra of all the  $\text{MgH}_2$  systems and  $\text{H}_2$ . On the other hand, for the  $\text{MgH}_2$  system we consider, it has been shown that even though H has a low mass, but the vibrational entropies for H in the lattice and in the  $\text{H}_2$  reservoir are rather similar and hence the net entropy difference is small.<sup>14</sup> Also we have used a relatively large supercell dimension so that the added defect charge density in the supercell is very low. Consequently, the interaction energy between the charged defects in the neighboring cells is expected to be sufficiently small, not to affect our conclusion.

The results above suggest the dominating defect and dopant species to be  $\text{V}_H^{+1}$ ,  $\text{Li}_{\text{Mg}}^{-1}$ , and  $\text{Li}_i^{+1}$ . However, we did not consider the interaction between  $\text{V}_H^{+1}$  and  $\text{Li}_{\text{Mg}}^{-1}$ . Next, we calculated the attractive interaction energy between  $\text{V}_H^{+1}$  and  $\text{Li}_{\text{Mg}}^{-1}$  as a function of their separation as shown in Fig. 2. We did not consider the interaction between  $\text{V}_H^{+1}$  and  $\text{Li}_i^{+1}$  because it is repulsive. Two key features are found in Fig. 2(b): (1)  $\text{V}_H^{+1}$  prefers to sit in one of the six nearest-neighbor H-sites (site 1 and site 2 in Fig. 2(a)) of Li with binding energy of 0.50–0.55 eV; (2) once beyond the nearest-neighbor H-site, their attraction decays rapidly to be insignificant. Based on this observation, we propose a nearest-neighbor interaction model to determine how many  $\text{V}_H^{+1}$  being trapped by  $\text{Li}_{\text{Mg}}^{-1}$  as a function of Li doping concentration. We assume that the interaction energy is  $\Delta E_b = -0.55$  eV when  $\text{V}_H^{+1}$  is in any of the six nearest-neighbor sites and negligible otherwise. Following the Boltzmann distribution,<sup>27</sup> we have

$$R_{\text{trapped}} = \frac{3n \exp[-\Delta E_b/k_B T]}{[2N - 3n] + 3n \exp[-\Delta E_b/k_B T]}, \quad (3)$$

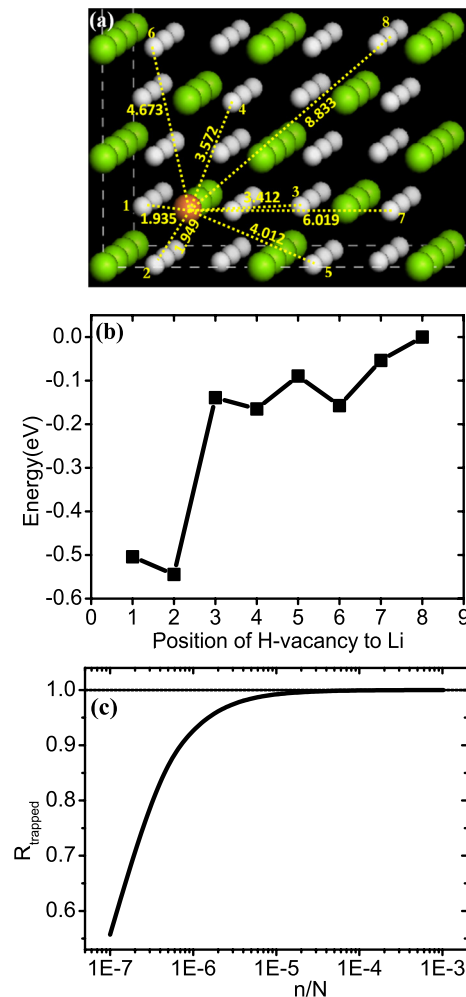


FIG. 2. (a) The structure of Li-dopant plus H-vacancy with H-vacancy at different positions labeled with number and distance from Li. (b) Interaction energy between  $\text{V}_H^{+1}$  and  $\text{Li}_{\text{Mg}}^{-1}$  as a function of their separation distance (in Angstrom). (c) Ratio of the trapped  $\text{V}_H^{+1}$  with  $\text{Li}_{\text{Mg}}^{-1}$  to the number of  $\text{V}_H^{+1}$ ,  $T = 400$  K. Green balls are Mg atoms, white balls are H atoms, and orange ball is Li dopant.

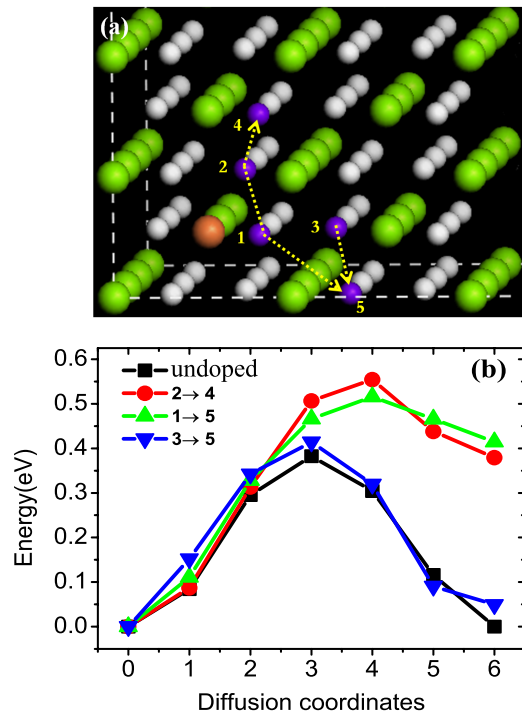


FIG. 3. (a) Illustration of different diffusion paths for  $V_H$  to diffuse away, further way from Li site. The arrow indicates diffusion direction. (b)  $V_H$  mediated H-diffusion barrier change with the presence of Li. The purple ball indicates the position of  $V_H$  in our calculation. The arrow indicates the diffusion path.

where  $R_{trapped}$  is the ratio of the number of trapped  $V_H^+$  to the total number of  $V_H^+$ ,  $n$  is the number of doped Li, and  $N$  is the number of Mg sites. The number of substitutional and interstitial Li is taken to the same under the charge-neutrality condition, as shown in Fig. 1.

Fig. 2(c) shows the calculated  $R_{trapped}$  as a function of Li doping concentration. We see that even in the low concentration (for example,  $\frac{n}{N} = 1 \times 10^{-4}$ ), the trapping ratio  $R_{trapped}$  is very close to one, indicating that almost all the  $V_H^+$  next to Li are immobilized due to their attractive interaction. This also indicates that H vacancy prefers to stay next to  $Li_{Mg}^{-1}$ , because its formation energy is effectively decreased by 0.55 eV.

Furthermore, we studied kinetically how H-vacancy diffusion is affected by the presence of  $Li_{Mg}$  through the calculation of diffusion barriers. In Fig. 3, we show the barriers for the H-vacancy diffusing from the nearest-neighbor sites of Li (sites 1 and 2 in Fig. 3(a)) to its closest H site (sites 4 and 5) (path 1) and from the next nearest-neighbor site (site 3) to its closet H site (site 5) (path 2). For the path 1, the diffusion barrier is found to increase by 0.15 eV compared to that in the undoped  $MgH_2$ . For the path 2, the diffusion barrier is found only  $\sim 30$  meV higher than that in the undoped  $MgH_2$ . This strong site dependence of H-vacancy diffusion barrier is consistent with the fast decay of the attractive interaction between  $V_H$  and  $Li_{Mg}$  as shown in Fig. 2(b). The 0.15 eV increase of diffusion barrier, together with the large  $V_H$  trapping ratio suggest that H vacancies will mostly be immobilized in the vicinity of Li dopants, inhibiting the  $V_H$  mediated H diffusion.

## IV. CONCLUSIONS

In conclusion, we have investigated the effects of Li-doping in  $MgH_2$  on the H-vacancy mediated H-diffusion, using DFT calculations. The formation energy calculation shows that the Li dopant favors two charged configurations of  $Li_{Mg}^{-1}$  and  $Li_i^{+1}$ . The charge neutrality condition requires the Fermi energy be shifted towards the VBM by 0.25 eV and 0.39 eV upon Li doping under the H-poor and H-rich conditions, respectively, which decreases the formation energy of  $V_H^+$  by the same amount. This leads to an increase of  $V_H^+$  concentration by up to about 5 orders of magnitude at  $T = 400$  K. Furthermore, the calculations of interaction energy between  $V_H^{+1}$  and  $Li_{Mg}^{-1}$  as well as diffusion barrier of H vacancy in the presence of Li show that almost all the H-vacancy next to Li are immobilized. Therefore, the H-diffusion is enhanced by Li doping in  $MgH_2$  only at the low Li doping concentration but not at the high concentration.

## ACKNOWLEDGMENTS

This work was supported by NSF MRSEC (Grant No. DMR-1121252) and DOE-BES (Grant No. DE-FG02-04ER46148). We thank the CHPC at University of Utah and NERSC for providing the computing resources.

- <sup>1</sup>P. Selvam, B. Viswanathan, C. S. Swamy, and V. Srinivasan, *Int. J. Hydrogen Energy* **11**, 169 (1986).
- <sup>2</sup>W. Klose and V. Stuke, *Int. J. Hydrogen Energy* **20**, 309 (1995).
- <sup>3</sup>F. H. Ellinger *et al.*, *J. Am. Chem. Soc.* **77**, 2647 (1955).
- <sup>4</sup>K. Zeng, T. Klassen, W. Oelerich, and R. Bormann, *Int. J. Hydrogen Energy* **24**, 989 (1999).
- <sup>5</sup>T. Noritake, M. Aoki, S. Towata, Y. Seno, and Y. Hirose, *Appl. Phys. Lett.* **81**, 2008 (2002).
- <sup>6</sup>B. Bogdanovi, K. Bohmhammel, B. Christ, A. Reiser, K. Schlichte, R. Vehlen, and U. Wolf, *J. Alloys Compd.* **282**, 84 (1999).
- <sup>7</sup>B. Sakintuna, F. Darkrim, and M. Hirscher, *Int. J. Hydrogen Energy* **32**, 1121 (2007).
- <sup>8</sup>M. Pozzo and A. Alfe, *Phys. Rev. B* **77**, 104103 (2008).
- <sup>9</sup>R. Yu and P. Lam, *Phys. Rev. B* **37**, 8730 (1988).
- <sup>10</sup>H. Reule, M. Hirscher, A. Weißhardt, and H. Kronmüller, *J. Alloys Compd.* **305**, 246 (2000).
- <sup>11</sup>N. Hanada, T. Ichigawa, and H. Fujii, *J. Phys. Chem. B* **109**, 7188 (2005).
- <sup>12</sup>P. Larsson, C. Araujo, J. Larsson, P. Jena, and R. Ahuja, *Proc. Natl. Acad. Sci. U.S.A.* **105**, 8227 (2008).
- <sup>13</sup>A. Baldi, M. Gonzalez-Silveira, V. Palmisano, B. Dam, and R. Griessen, *Phys. Rev. Lett.* **102**, 226102 (2009).
- <sup>14</sup>A. Peles and C. Van de Walle, *Phys. Rev. B* **76**, 214101 (2007).
- <sup>15</sup>S. Hao and D. Sholl, *Appl. Phys. Lett.* **93**, 251901 (2008).
- <sup>16</sup>N. Umezawa, M. Sato, and K. Shiraishi, *Appl. Phys. Lett.* **93**, 223104 (2008).
- <sup>17</sup>S. Hao and D. Sholl, *Appl. Phys. Lett.* **94**, 171909 (2009).
- <sup>18</sup>M. Park, A. Janotti, and C. Van de Walle, *Phys. Rev. B* **80**, 064102 (2009).
- <sup>19</sup>K. Hoang and C. Van de Walle, *Phys. Rev. B* **80**, 214109 (2009).
- <sup>20</sup>K. Smith, T. Fisher, U. Waghmare, and R. Crespo, *Phys. Rev. B* **82**, 134109 (2010).
- <sup>21</sup>G. Kresse and D. Joubert, *Phys. Rev. B* **59**, 1758 (1999).
- <sup>22</sup>J. P. Perdew, J. A. Chevary, S. H. Vosko, K. A. Jackson, M. R. Pederson, D. J. Singh, and C. Fiolhairs, *Phys. Rev. B* **46**, 6671 (1992).
- <sup>23</sup>G. Kresse and J. Furthmüller, *Phys. Rev. B* **54**, 11169 (1996).
- <sup>24</sup>G. Mills and H. Jonsson, *Phys. Rev. Lett.* **72**, 1124 (1994).
- <sup>25</sup>C. Van de Walle and J. Neugebauer, *J. Appl. Phys.* **95**, 3851 (2004).
- <sup>26</sup>S. Na-Phattalung, M. J. Smith, K. Kim, M. H. Du, S. H. Wei, S. B. Zhang, and S. Limpitjumnong, *Phys. Rev. B* **73**, 125205 (2006).
- <sup>27</sup>G. H. Lu, Q. Wang, and F. Liu, *Appl. Phys. Lett.* **92**, 211906 (2008).